




## Research Article

# Joint Doppler Shift and Channel Estimation for High-Speed Railway Wireless Communications in Tunnel Scenarios

Zhigang Wang <sup>1</sup>, Zihao Wang,<sup>2</sup> Fusheng Zhu <sup>1</sup>, Zezhou Luo,<sup>1</sup>  
Fang Li <sup>1</sup> and Haopeng Liu<sup>3</sup>

<sup>1</sup>Guangdong Communications and Networks Institute, Guangzhou, Guangdong, China

<sup>2</sup>School of Mechanics and Civil Engineering, China University of Mining and Technology, Xuzhou, Jiangsu, China

<sup>3</sup>Institute of Computing Technologies, China Academy of Railway Sciences Corporation Limited, Beijing 100081, China

Correspondence should be addressed to Zhigang Wang; wangzhigang@gdcni.cn

Received 8 October 2021; Accepted 6 December 2021; Published 31 January 2022

Academic Editor: Li Zhu

Copyright © 2022 Zhigang Wang et al. This is an open access article distributed under the Creative Commons Attribution License, which permits unrestricted use, distribution, and reproduction in any medium, provided the original work is properly cited.

In this work, we study the problem of Doppler shift and channel estimation for wireless communication systems on high-speed railways (HSRs). We focus on tunnel scenario, one of the classical scenarios of HSRs. We first build up the mathematical system model, design a joint Doppler shift and channel estimator, and compare its performance with the typical Moose algorithm. We show that our estimator outperforms the Moose algorithm in Doppler estimation. Besides, since wireless channels in tunnel scenarios often contain several or multiple taps, we suggest an adaptive frame structure to improve transmission efficiency. Simulations are then provided to corroborate our proposed studies.

## 1. Introduction

During the past two decades, Chinese government has obtained a world famous achievement: the fast development and deployment of high-speed rails (HSRs) [1]. By the end of 2020, almost 40,000 kilometers of HSRs have been built in the vast mainland of China. HSRs greatly boost the economy and significantly change the lives of people.

Accordingly, research and applications of wireless communications on HSRs arouse extensive interests [2, 3]. Different from other scenarios of wireless communication systems, the scenario of HSRs has three special features:

- (1) High mobility of train
- (2) Large penetration loss of the signals passing through train carriages [4]
- (3) Access requirement of large users within a short period

The three special characteristics give rise to a series of research challenges for the wireless communications on HSRs, including channel modeling, Doppler shift compensation, time-varying channel estimation, fast handover,

large and quick access methods, adaptive beamforming, and signal detection [1, 2, 5]. Besides, the applications and future visions of the 5th and 6th generation technologies on HSRs, such as massive multiple input multiple output (massive MIMO) [4], millimeter-wave (mmWave) [6], visible light communications, reconfigurable intelligent surfaces, newly emergent backscatter communications [7, 8], and smartly connected world, also bring about new open challenges for both academic research and engineering realization [9, 10].

High mobility will result in Doppler shifts that can cause channels to be fast time-varying [11, 12]. Doppler shifts can destroy the orthogonality of subcarriers of orthogonal frequency division multiplexing (OFDM) systems [13]. Therefore, estimation and compensation of Doppler shifts are of vital importance for wireless OFDM systems.

The most famous Doppler shift estimator is the Moose algorithm proposed by Moose in 1994 [14]. It requires the transmitter to send two identical OFDM symbols, and the receiver uses the difference of the received signals to estimate the CFO, that is, the Moose algorithm exploits the fact that each subcarrier in the frequency domain has the same phase frequency shift.

Based on the Moose algorithm, Schmidl and Cox presented another CFO estimator in 1997 [15]. They divided the frequency offset into fractional and integer multiples, used the relation of two identical parts of an OFDM symbol, and defined two symbols with a specific pilot format to estimate the fractional and integer multiple frequency offset separately.

In 1999, Morelli and Mengali proposed the Morelli-Mengali (MM) algorithm [16]. It supposes the transmitter transmits several same signals, and the receiver divides the received information into identical parts and then calculates the autocorrelation between the parts, so as to construct the linear relationship between the autocorrelation and the frequency offset. After that, the frequency offset is estimated by a specially designed best linear unbiased estimation algorithm.

If the Doppler shift cannot be compensated or there exists a difference between the transmitter oscillator and receiver oscillator, the channels will become time-varying [17–21]. In such cases, time-varying channel estimators can be applied which transfer many channel parameters into a few parameters through basis expansion models (BEMs) [22–24], autoregressive models [25, 26], array signal processing models [27, 28], or exploiting channel sparse feature [21, 29].

Tunnels are one of the classic scenarios of HSRs. It is known that the wireless channels in tunnel scenarios are rich of taps, that is, multiple wireless paths often exist in tunnels on HSRs [30]. Recently, it is revealed that if the base station (BS) is located in the middle of a tunnel, there are more wireless paths in the both ends of the tunnel than those in the middle of the tunnel [31]. Such feature arouses our interest and motivates this study.

In this study, we focus on the tunnel scenarios and investigate the Doppler shift and channel estimation problems for wireless OFDM communication systems. Specifically, we build up the mathematical system model, exploit the feature of wireless channels in tunnel scenarios, design a joint Doppler shift and channel estimator, and compare its performance with the typical Moose algorithm.

The rest of the study is organized as follows. Section 2 introduces the mathematical system model. Section 3 designs a joint Doppler shift and channel estimator. Section 4 provides simulation results to corroborate the proposed studies, and Section 5 summarizes the whole study.

Notations: vectors and matrices are boldface small and capital letters; the transpose, Hermitian, inverse, and pseudoinverse of the matrix  $\mathbf{A}$  are denoted by  $\mathbf{A}^T$ ,  $\mathbf{A}^H$ ,  $\mathbf{A}^{-1}$ , and  $\mathbf{A}^\dagger$ , respectively;  $\text{diag}\{\mathbf{a}\}$  denotes a diagonal matrix with the diagonal elements constructed from  $\mathbf{a}$ ,  $E\{\cdot\}$  denotes the statistical expectation,  $\lceil \cdot \rceil$  is the integer ceiling, and the entry indices of vectors and matrices start from 1.

## 2. System Model

Consider the wireless communication system in the tunnel, as shown in Figure 1. The system consists of a transmitter with one base station (BS) antenna and a receiver with one train antenna.

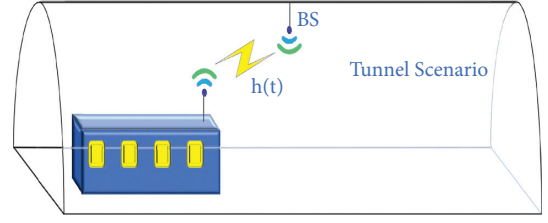


FIGURE 1: System model.

Suppose BS transmits OFDM symbols to the train antenna. Each OFDM symbol contains  $N$  discrete signals  $s(n)$ ,  $1 \leq n \leq N$ , and duration of each signal is  $T_s$ . Define  $\mathbf{s} = [s(0), s(1), \dots, s(N-1)]^T$ . After inverse Fourier transform, we can have  $\mathbf{x} = \mathbf{F}^H \mathbf{s}$ , where  $\mathbf{F}$  represents the discrete Fourier transform matrix.

The BS modulates the signals  $\mathbf{x}$  to the carrier frequency  $f_{c0}$  and transmits them via the antenna, that is, the BS will transmit the analog signals:

$$b(t) = x(t)e^{j(2\pi f_{c0}t + \theta_0)}, \quad (1)$$

where  $\theta_0$  denotes the initial phase of the transmitter oscillator [32].

Assume that the fading channels between the BS antenna and the train antenna is  $h(t)$ . The received signals at the train antenna can be obtained as

$$\begin{aligned} r(t) &= h(t)e^{j2\pi f_d t} * b(t) + w(t) \\ &= h(t) * x(t)e^{j(2\pi(f_{c0} + f_d)t + \theta_0)} + w(t), \end{aligned} \quad (2)$$

where  $w(t)$  denotes the white Gaussian noise.

The first step for the receiver is to down-convert the signals  $r(t)$  to the baseband signals, which is given by

$$y(t) = r(t)e^{-j(2\pi f_{c1}t + \theta_1)}, \quad (3)$$

where  $f_{c1}$  is the carrier frequency of the receiver oscillator, and  $\theta_1$  denotes its initial phase.

Substituting (2) into (3), we can further obtain

$$y(t) = h(t) * x(t)e^{j(2\pi(f_{c0} - f_{c1} + f_d)t + (\theta_0 - \theta_1))} + w(t). \quad (4)$$

Define

$$g(t) = h(t)e^{j(\theta_0 - \theta_1)}. \quad (5)$$

In the case of  $f_{c0} = f_{c1}$ , i.e., the transmitter and the receiver are of the same carrier frequency, and we can rewrite (4) as

$$y(t) = e^{j2\pi f_d t} g(t) * x(t) + w(t). \quad (6)$$

Clearly, our goal is to estimate the Doppler shift  $f_d$  and the channels  $g(t)$ , which is the focus of our next section.

*Remark 1.* The CFO is defined as

$$v = f_{c0} - f_{c1} + f_d, \quad (7)$$

which indicates that two factors can result in CFO: (1) the Doppler shift  $f_d$  caused by movement of the transceiver; (2)

the difference  $f_{c0} - f_{c1}$  between the transmitter oscillator and the receiver oscillator.

### 3. Joint Doppler Shift and Channel Estimator

This section aims to design a joint Doppler shift and channel estimator to estimate  $f_d$  and  $g(t)$ .

*3.1. Channel Coherence Time.* When the train speed  $v_t$  is 360 km/hour, i.e.,  $v_t = 100$  m/s, we can find the maximum Doppler shift:

$$\max f_d = \frac{v_t}{\lambda} = \frac{v_t}{c/f_{c0}}, \quad (8)$$

where  $\lambda$  denotes the wavelength and  $c = 3 * 10^8$  m/s. In the case of  $f_{c0} = 3 * 10^9$ , we can find  $\max f_d = 1000$  Hz. Accordingly, the channel coherence time  $T_c$  is

$$T_c = \frac{1}{2 \max f_d} = 5 * 10^{-4}, \quad (9)$$

which indicates that during the period of 0.5 ms, and the channels between the BS antenna and the train antenna can be considered as static or quasistatic.

*3.2. Design of Joint Estimator.* Suppose the channels  $g(t)$  contains  $L$  taps, that is, the channels  $g(t) = 0$  when  $t \geq LT_s$ . After sampling, we can obtain (6) as

$$\begin{aligned} y(nT_s) &= y(t)|_{t=nT_s} \\ &= e^{j2\pi f_d nT_s} \sum_{l=0}^{L-1} g_l x(nT_s - lT_s) + w(nT_s), \end{aligned} \quad (10)$$

where  $0 \leq n \leq N - 1$  and

$$g(lT_s) = g_l, \quad 0 \leq l \leq L - 1. \quad (11)$$

For conciseness, we assume  $T_s = 1$  and can further have

$$y(n) = e^{j2\pi f_d n} \sum_{l=0}^{L-1} g_l x(n-l) + w(n). \quad (12)$$

Define

$$\begin{aligned} \mathbf{y} &= [y(0), y(1), \dots, y(N-1)]^T, \\ \mathbf{x} &= [x(0), x(1), \dots, x(N-1)]^T, \\ \mathbf{w} &= [w(0), w(1), \dots, w(N-1)]^T, \end{aligned} \quad (13)$$

$$\Gamma(f_d) = \text{diag}\{1, e^{j2\pi f_d}, e^{j2\pi 2f_d}, \dots, e^{j2\pi(N-1)f_d}\}.$$

We can rewrite (12) as

$$\mathbf{y} = \Gamma(f_d) \mathbf{G} \mathbf{x} + \mathbf{w}, \quad (14)$$

where  $\mathbf{G}$  is the circulant matrix.

$$\mathbf{G} = \begin{bmatrix} g_0 & 0 & \cdots & 0 & g_{L-1} & \cdots & g_1 \\ g_1 & g_0 & \cdots & 0 & 0 & \cdots & g_2 \\ \vdots & \vdots & \cdots & \vdots & \vdots & \cdots & \vdots \\ g_{L-1} & g_{L-2} & \cdots & g_0 & 0 & \cdots & 0 \\ 0 & g_{L-1} & g_{L-2} & \cdots & g_0 & \cdots & 0 \\ \vdots & \vdots & \cdots & \vdots & \vdots & \cdots & \vdots \\ 0 & 0 & g_{L-1} & g_{L-2} & \cdots & \cdots & g_0 \end{bmatrix}. \quad (15)$$

Suppose

$$\begin{aligned} \mathbf{g} &= [g_0, g_1, \dots, g_{L-1}]^T, \\ \bar{\mathbf{g}} &= \left[ \mathbf{g}^T, \underbrace{0, 0, \dots, 0}_{N-L} \right]^T. \end{aligned} \quad (16)$$

It can be readily checked that

$$\mathbf{G} = \mathbf{F}^H \mathbf{D} \mathbf{F}, \quad (17)$$

where

$$\mathbf{D} = \text{diag}\{\mathbf{d}\} = \text{diag}\{\mathbf{F} \mathbf{g}\}. \quad (18)$$

Since  $\Gamma(f_d) \Gamma(-f_d) = \mathbf{I}$ , we can rewrite (14) as

$$\Gamma(-f_d) \mathbf{y} = \mathbf{G} \mathbf{x} + \Gamma(-f_d) \mathbf{w}. \quad (19)$$

Substituting (17) into (19) and using  $\mathbf{F}^H \mathbf{F} = \mathbf{I}$  and  $\mathbf{x} = \mathbf{F}^H \mathbf{s}$ , we can obtain

$$\begin{aligned} \Gamma(-f_d) \mathbf{y} &= \mathbf{F}^H \mathbf{D} \mathbf{F} \mathbf{x} + \Gamma(-f_d) \mathbf{w} \\ &= \mathbf{F}^H \mathbf{D} \mathbf{F} \mathbf{F}^H \mathbf{s} + \Gamma(-f_d) \mathbf{w} \\ &= \mathbf{F}^H \mathbf{D} \mathbf{s} + \Gamma(-f_d) \mathbf{w}. \end{aligned} \quad (20)$$

Multiplying both sides of equation (20) with  $\mathbf{F}$  will produce

$$\mathbf{F} \Gamma(-f_d) \mathbf{y} = \mathbf{D} \mathbf{s} + \tilde{\mathbf{w}}, \quad (21)$$

where

$$\tilde{\mathbf{w}} = \mathbf{F} \Gamma(-f_d) \mathbf{w}. \quad (22)$$

Define

$$\mathbf{z} = \mathbf{F} \Gamma(-f_d) \mathbf{y}. \quad (23)$$

It is worth noting that the vector  $\mathbf{z}$  contains only one unknown parameter  $f_d$ . We can have

$$\mathbf{z} = \mathbf{D} \mathbf{s} + \tilde{\mathbf{w}} = \mathbf{S} \mathbf{d} + \tilde{\mathbf{w}}, \quad (24)$$

$$= \mathbf{S} \mathbf{F} \mathbf{g} + \tilde{\mathbf{w}}, \quad (25)$$

where  $\mathbf{d} = \text{diag}(\mathbf{D}) = \mathbf{F} \mathbf{g}$ .

Suppose the number of pilots in one OFDM symbol is  $M$  and the pilot order in the OFDM symbol is  $\{p_0, p_1, \dots, p_{M-1}\}$ . We choose the following symbols from (25) and construct the following new vectors and matrixes:

$$\begin{aligned}
\mathbf{z}_p &= [\mathbf{z}(p_0), \mathbf{z}(p_1), \dots, \mathbf{z}(p_{M-1})]^T, \\
\mathbf{s}_p &= [\mathbf{s}(p_0), \mathbf{s}(p_1), \dots, \mathbf{s}(p_{M-1})]^T, \\
\mathbf{d}_p &= [\mathbf{d}(p_0), \mathbf{d}(p_1), \dots, \mathbf{d}(p_{M-1})]^T, \\
\tilde{\mathbf{w}}_p &= [\tilde{\mathbf{w}}(p_0), \tilde{\mathbf{w}}(p_1), \dots, \tilde{\mathbf{w}}(p_{M-1})]^T.
\end{aligned} \tag{26}$$

Therefore, we can have

$$\mathbf{z}_p = \mathbf{S}_p \mathbf{d}_p + \tilde{\mathbf{w}}_p, \tag{27}$$

where  $\mathbf{S}_p = \text{diag}\{\mathbf{s}_p\}$ .

It is worth noting that the matrix  $F$  is square and orthogonal. Let us choose the first  $L$  columns and  $M$  rows of  $F$  as  $\mathbf{F}_p$

$$\mathbf{F}_p = \mathbf{F}(1: M, 1: L). \tag{28}$$

Then, we can obtain

$$\mathbf{d}_p = \mathbf{F}_p \mathbf{g}. \tag{29}$$

Substituting (29) into (27), we can find

$$\mathbf{z}_p = \mathbf{S}_p \mathbf{F}_p \mathbf{g} + \tilde{\mathbf{w}}_p. \tag{30}$$

Accordingly, our estimator aims to obtain

$$\{\hat{f}_d, \hat{\mathbf{g}}\} = \arg \min |\mathbf{z}_p - \mathbf{S}_p \mathbf{F}_p \mathbf{g}|^2. \tag{31}$$

It can be readily checked that

$$\hat{\mathbf{g}} = (\mathbf{F}_p^H \mathbf{S}_p \mathbf{F}_p)^{-1} \mathbf{F}_p^H \mathbf{S}_p \mathbf{z}_p. \tag{32}$$

Subsequently, the Doppler shift  $f_d$  can be estimated through one-dimensional search:

$$\{\hat{f}_d\} = \arg \min |\mathbf{z}_p - \mathbf{S}_p \mathbf{F}_p (\mathbf{F}_p^H \mathbf{S}_p \mathbf{F}_p)^{-1} \mathbf{F}_p^H \mathbf{S}_p \mathbf{z}_p|^2. \tag{33}$$

Next, we can estimate  $\mathbf{g}$  using (32).

With estimated  $\hat{\mathbf{g}}$ , we can recover the matrix using (18).

*Remark 2.* The receiver will discard the cyclic prefix (CP) part as shown in Figure 2. It is worth noting that the length of the CP part can be changed so as to achieve adaptive transmission. In the places where less wireless paths exist, for example, the middle of the tunnel, the CP contains less symbols, while the CP will include more symbols in the case of multiple paths.

## 4. Simulation Results

This section provides numerical examples to evaluate the proposed studies. Here, we set  $N = 512$ , unless otherwise specified. We assume that the channel  $g_l$  follows Rayleigh distribution.

We use the simulation platform CloudRT, a ray-tracing channel simulation platform, to generate the wireless channels in tunnels and investigate the feature of channels (CloudRT is a high performance computing (HPC) cloud-based platform. More details can be found in the website <https://www.raytracer.cloud>).

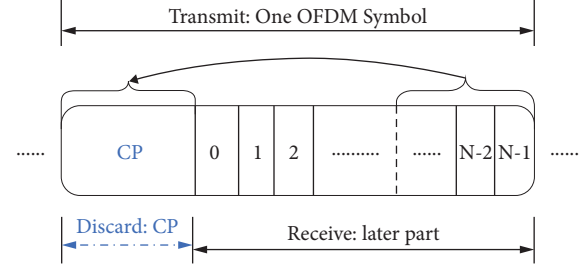


FIGURE 2: Structure of one OFDM symbol.

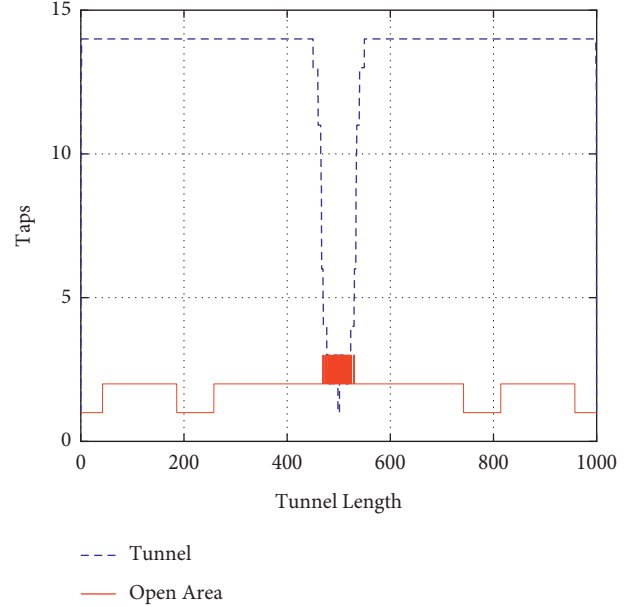


FIGURE 3: Channel taps of tunnels and open area.

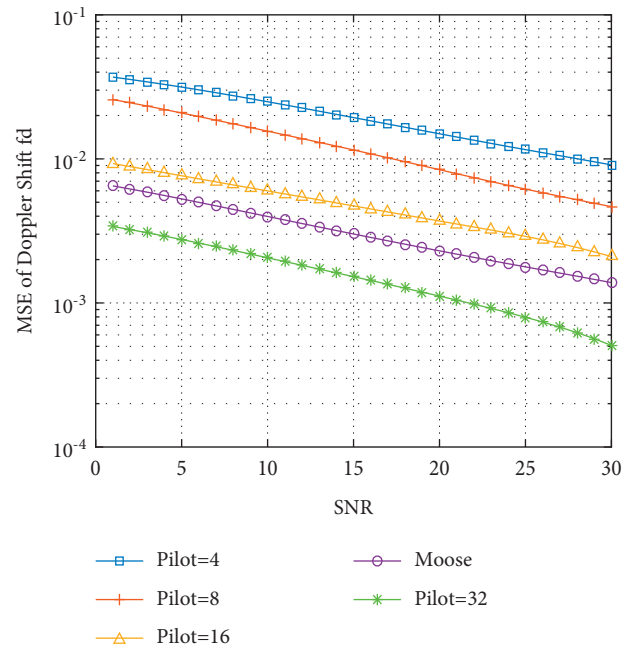


FIGURE 4: Estimation MSE of the Doppler shift.

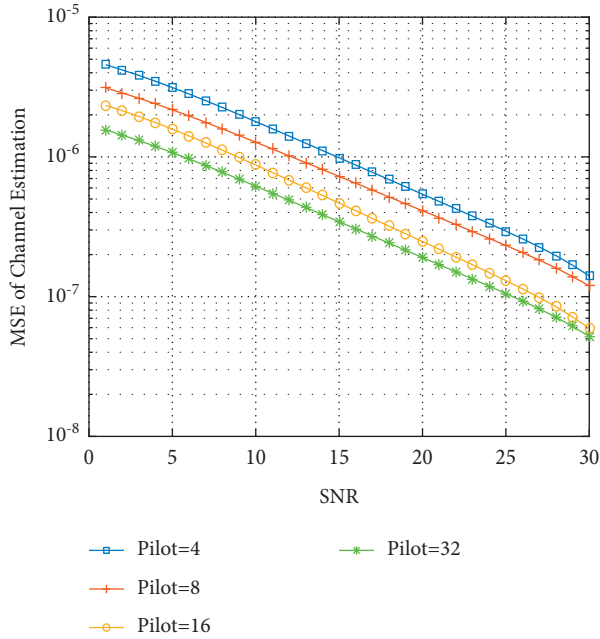


FIGURE 5: Estimation MSE of the channels.

Figure 3 shows the channel taps of two scenarios: tunnels and open areas. Our BS is located in the middle of the tunnel, i.e., 500 m of the tunnel length. It can be seen from Figure 3 that the number of channels taps is more than 10 at both ends of the tunnel while only about 2 taps at the middle of the tunnel, which is a sharp contrast to the open area scenario that only has 2 or 3 paths.

Figure 4 shows the Doppler estimation MSEs of our estimator. For comparison, the MSE of the Moose algorithm is also provided. It can be seen from Figure 4 that our joint estimator outperforms the Moose algorithm and that more pilots can enhance the estimation accuracy.

Figure 5 shows the channel estimation MSEs of our estimator. We set number of pilots as 4, 8, 16, and 32 separately. It can be found from Figure 5 that more pilots can result in better estimation performance.

## 5. Conclusion

We focused on the tunnels, a classic scenario of HSRs, and investigated the Doppler shift and channel estimation problems. Specifically, we built up the mathematical model for the wireless OFDM system in tunnels, designed a joint Doppler shift and channel estimation algorithm, and compared its performance with the typical Moose algorithm. It is found that our estimator could outperform the Moose algorithm in Doppler estimation and that more pilots would achieve better estimation performance. Finally, simulations were provided to corroborate our proposed studies.

## Data Availability

The data used to support the findings of this study are available from the corresponding author upon request.

## Conflicts of Interest

The authors declare that there are no conflicts of interest.

## Acknowledgments

This work was funded by Key-Area Research and Development Program of Guangdong Province (2018B010124001).

## References

- [1] B. Ai, A. F. Molisch, M. Rupp, and Z.-D. Zhong, "5G key technologies for smart railways," *Proceedings of the IEEE*, vol. 108, no. 6, pp. 856–893, 2020.
- [2] B. Ai, C. Briso-Rodriguez, X. Cheng et al., "Challenges toward wireless communications for high-speed railway," *IEEE Transactions on Intelligent Transportation Systems*, vol. 15, no. 5, pp. 2143–2158, 2014.
- [3] W. Zhou, J. Wu, and P. Fan, "High mobility wireless communications with doppler diversity: fundamental performance limits," *IEEE Transactions on Wireless Communications*, vol. 14, no. 12, pp. 6981–6992, 2015.
- [4] R. He, C. Schneider, B. Ai et al., "Propagation channels of 5G millimeter wave vehicle-to-vehicle communications: recent advances and future challenges," *IEEE Vehicular Technology Magazine*, vol. 5, no. 1, 2019.
- [5] L. Zhu, H. Liang, H. Wang, B. Ning, and T. Tang, "Joint security and train control design in blockchain empowered CBTC system," *IEEE Internet of Things Journal*, 2021.
- [6] R. He, B. Ai, G. L. Stuber, G. Wang, and Z. Zhong, "Geometrical-based modeling for millimeter-Wave MIMO mobile-to-mobile channels," *IEEE Transactions on Vehicular Technology*, vol. 67, no. 4, pp. 2848–2863, 2018.
- [7] G. Wang, F. Gao, R. Fan, and C. Tellambura, "Ambient backscatter communication systems: detection and performance analysis," *IEEE Transactions on Communications*, vol. 64, no. 11, pp. 4836–4846, 2016.
- [8] W. Zhao, G. Wang, B. Ai, J. Li, and C. Tellambura, "Backscatter aided wireless communications on high-speed rails: capacity analysis and transceiver design," *IEEE Journal on Selected Areas in Communications*, vol. 38, no. 12, pp. 2864–2874, 2020.
- [9] Z. Zhang, X. Chai, K. Long, A. V. Vasilakos, and L. Hanzo, "Full-duplex techniques for 5G networks: self-interference cancellation, protocol design and relay selection," *IEEE Communications Magazine*, vol. 53, no. 5, pp. 128–137, 2015.
- [10] Y. Li, L. Zhu, H. Wang, F. R. Yu, and S. Liu, "A cross-layer defense scheme for edge intelligence-enabled CBTC systems against MitM attacks," *IEEE Transactions on Intelligent Transportation Systems*, vol. 22, no. 4, pp. 2286–2298, 2021.
- [11] G. Wang, Q. Liu, R. He, F. Gao, and C. Tellambura, "Acquisition of channel state information in heterogeneous cloud radio access networks: challenges and research directions," *IEEE Wireless Communications*, vol. 22, no. 3, pp. 100–107, 2015.
- [12] T. Li, X. Wang, P. Fan, and T. Riihonen, "Position-aided large-scale MIMO channel estimation for high-speed railway communication systems," *IEEE Transactions on Vehicular Technology*, vol. 66, no. 10, pp. 8964–8978, 2017.
- [13] L. Yang, G. Ren, and Z. Qiu, "A novel Doppler frequency offset estimation method for DVB-T system in HST environment," *IEEE Transactions on Broadcasting*, vol. 58, no. 1, pp. 139–143, 2012.

- [14] P. H. Moose, "A technique for orthogonal frequency division multiplexing frequency offset correction," *IEEE Transactions on Communications*, vol. 42, no. 10, pp. 2908–2914, 1994.
- [15] T. M. Schmidl and D. C. Cox, "Robust frequency and timing synchronization for OFDM," *IEEE Transactions on Communications*, vol. 45, no. 12, pp. 1613–1621, 1997.
- [16] M. Morelli and U. Mengali, "An improved frequency offset estimator for OFDM applications," *IEEE Communications Letters*, vol. 3, no. 3, pp. 75–77, 1999.
- [17] J. You, Z. Zhong, Z. Dou, J. Dang, and G. Wang, "Wireless relay communication on high speed railway: full duplex or half duplex?" *China Communications*, vol. 13, no. 11, pp. 14–26, 2016.
- [18] S. Zhang, F. Gao, H. Wang, and C. Pei, "Dynamic individual channel estimation for one-way relay networks with time-multiplexed-superimposed training," *IEEE Transactions on Vehicular Technology*, vol. 63, no. 8, pp. 3841–3852, 2014.
- [19] X. Xie, M. Peng, F. Gao, and W. Wang, "Superimposed training based channel estimation for uplink multiple access relay networks," *IEEE Transactions on Wireless Communications*, vol. 14, no. 8, pp. 4439–4453, 2015.
- [20] S. Zhang, F. Gao, J. Li, and M. Sheng, "Online and offline bayesian cramer-rao bounds for time-varying channel estimation in one-way relay networks," *IEEE Transactions on Signal Processing*, vol. 63, no. 8, pp. 1977–1992, 2015.
- [21] J. Ma, S. Zhang, H. Li, F. Gao, and S. Jin, "Sparse bayesian learning for the time-varying massive MIMO channels: acquisition and tracking," *IEEE Transactions on Communications*, vol. 67, no. 3, pp. 1925–1938, 2019.
- [22] S. Zhang, F. Gao, J. Li, and H. Li, "Time varying channel estimation for dstc-based relay networks: tracking, smoothing and BCRBs," *IEEE Transactions on Wireless Communications*, vol. 14, no. 9, pp. 5022–5037, 2015.
- [23] Y. Yang, F. Gao, X. Ma, and S. Zhang, "Deep learning-based channel estimation for doubly selective fading channels," *IEEE Access*, vol. 7, pp. 36579–36589, 2019.
- [24] X. Ma, G. B. Giannakis, and S. Ohno, "Optimal training for block transmissions over doubly selective wireless fading channels," *IEEE Transactions on Signal Processing*, vol. 51, no. 5, pp. 1351–1366, 2003.
- [25] M. Dong, L. Tong, and B. M. Sadler, "Optimal insertion of pilot symbols for transmissions over time-varying flat fading channels," *IEEE Transactions on Signal Processing*, vol. 52, no. 5, pp. 1403–1418, 2004.
- [26] M. Li, S. Zhang, N. Zhao, W. Zhang, and X. Wang, "Time-Varying massive MIMO channel estimation: capturing, reconstruction, and restoration," *IEEE Transactions on Communications*, vol. 67, no. 11, pp. 7558–7572, 2019.
- [27] Y. Ge, W. Zhang, F. Gao, S. Zhang, and X. Ma, "Beamforming network optimization for reducing channel time variation in high-mobility massive MIMO," *IEEE Transactions on Communications*, vol. 67, no. 10, pp. 6781–6795, 2019.
- [28] L. Zhu, Y. Li, F. R. Yu, B. Ning, T. Tang, and X. Wang, "Cross-layer defense methods for jamming-resistant CBTC systems," *IEEE Transactions on Intelligent Transportation Systems*, vol. 22, no. 11, pp. 7266–7278, 2021.
- [29] H. Xie, F. Gao, S. Zhang, and S. Jin, "A unified transmission strategy for TDD/FDD massive MIMO systems with spatial basis expansion model," *IEEE Transactions on Vehicular Technology*, vol. 66, no. 4, pp. 3170–3184, 2017.
- [30] R. He, B. Ai, G. Wang et al., "High-speed railway communications: from GSM-R to LTE-R," *IEEE Vehicular Technology Magazine*, vol. 11, no. 3, pp. 49–58, 2016.
- [31] R. He, B. Ai, G. Wang, M. Yang, C. Huang, and Z. Zhong, "Wireless channel sparsity: measurement, analysis, and exploitation in estimation," *IEEE Wireless Communications*, vol. 28, no. 4, pp. 113–119, 2021.
- [32] Y. Guo, G. Wang, R. Xu, R. He, X. Wei, and C. Tellambura, "Capacity analysis for wireless symbiotic communication systems with BPSK tags under sensitivity constraint," *IEEE Communications Letters*, vol. 26, no. 1, 2021.